*J. Fluid Mech.* (1984), *vol.* 143, *pp.* 153–172
*Printed in Great Britain*



# An experimental study of the mechanism of intermittent separation of a turbulent boundary layer

By QING-DING WEI
Department of Mechanics, Beijing University, Beijing, China

AND HIROSHI SATO
Institute of Interdisciplinary Research, University of Tokyo, Komaba, Meguro-ku, Tokyo, Japan

(Received 27 April 1983 and in revised form 30 January 1984)

A wind-tunnel investigation was made of the mechanism of separation of a two-dimensional turbulent boundary layer on a convex wall. The flow field was observed visually by using a large number of smoke wires arranged in various ways. Statistical quantities were obtained by newly developed direction-sensitive hot-wire probes and flow-direction meters. Smoke pictures show localized backflow spots in the separation region. They occur intermittently, grow downstream, merge with each other and eventually cover the whole flow field. Measurements of instantaneous flow direction show that velocity fluctuations in the separation region are strongly three-dimensional. The backflow factor, which is defined as the fraction of time of occurrence of backflow, is used for the quantitative description of the separation region. The role of large-scale ordered motions in the turbulent separation was investigated by use of the conditional sample and average technique. It was confirmed that a localized backflow is initiated by a large-scale low-speed lump of fluid which travels downstream.

## 1. Introduction

The separation of a laminar boundary layer in an adverse pressure gradient has been investigated extensively and well documented. It is now possible to predict the separation point to adequate accuracy. On the other hand, the separation of a turbulent boundary layer has not yet been clarified, although it is more important than laminar separation in most practical applications. Research on turbulent separation inclues two approaches. One is to accumulate massive experimental data on separation under various conditions and construct appropriate mathematical models for the prediction of separation. Predictions have been tried using various methods and applied to practical problems with partial success. The other approach is to elucidate the mechanism of separation by means of detailed measurements under simple conditions. The present study belongs to the latter category.

It has been pointed out the turbulent separation takes place intermittently (Sandborn & Kline 1961). It is also localized in space. This intermittency is one of the most important features of turbulent separation. Recently, detailed measurements were made by Simpson, Strickland & Barr (1977), Simpson, Chew & Shivaprasad (1981*a*, *b*) and Shiloh, Shivaprasad & Simpson (1981). They provided numerous data

on various statistical quantities, but the mechanism of the intermittent separation is not yet fully clear.

We realize that for detailed discussions we have to make clear what we mean by 'separation'. Although the word is widely used, a precise definition of turbulent separation seems to be impossible. Therefore we do not use the word in a quantitative sense. In order to describe quantitatively what happens in the flow we use the well-defined quantity 'backflow'. This simply means that an instantaneous flow vector has a component opposite to the main stream. Then the so-called intermittent separation is considered to be an intermittent occurrence of the backflow.

The objective of the present study is twofold. One purpose is to collect detailed data inside and outside the separation region. We measure statistical quantities of the velocity fluctuation and take pictures of the instantaneous flow field. From these data we can deduce what happens in the separation region. The second objective is to clarify the relationship between the large-scale ordered motion in the turbulent boundary layer and the occurrence of localized backflow. There is a strong possibility that the ordered motion is the cause of the intermittent backflow. If we can prove this, the mechanism of turbulent separation becomes very clear.

There are two kinds of arrangement for separation experiments. One is with reattachment and the other is without it. An example of the former is the backward-facing step and an example of the latter is the flow around a cylinder at high Reynolds numbers. The separation without reattachment is more complicated, because the flow field includes the wake. The occurrence of backflow might be influenced by the fluctuation in the wake. Therefore we have chosen an arrangement in which the flow separates on a convex wall and attaches to the wall again downstream. The occurrence of backflow was measured by newly developed hot-wire probes and observed by using a large number of smoke wires.

## 2. Experimental arrangements

### 2.1. *Wind tunnel*

Experiments were carried out in the Environmental Wind Tunnel of the University of Tokyo. The wind tunnel is of open-circuit blow-out type with a test section of 1 m by 1 m cross-section and 5 m length. The wind tunnel is equipped with a generator of arbitrary velocity and temperature distributions. Although the present experiment was carried out with uniform velocity and temperature distributions, the generator produced a fluctuation of about 2 % in the test section. The effect of the fluctuation on the separation seems to be negligible, because the intensity is small compared with that of the maximum fluctuation in the boundary layer of more than 10 %.

A flat plate 1.9 m in length was installed horizontally in the central plane of the test section as shown in figure 1. A tripwire 0.4 cm in diameter was attached to the plate 5 cm from the leading edge. A two-dimensional turbulent boundary layer was formed on the rear part of the plate. The plate is followed smoothly by a convex plate whose shape is expressed by a parabola $y = 20 - 0.008x^2$ in centimetre units. The turbulent boundary layer separates on the curved plate owing to the adverse pressure gradient and the centrifugal force. The convex plate is connected to another horizontal flat plate at the downstream end. The separated layer reattaches to the rear flat plate and forms a boundary layer again.

The $x$-axis is taken in the streamwise direction and the $y$-axis is taken normal to the flat plate as shown in figure 1. The distance in the $y$-direction from the surface

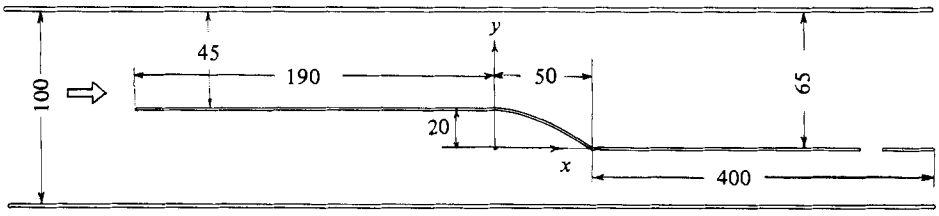


FIGURE 1. Experimental arrangement in the test section; lengths in cm.

of the curved plate is denoted by $y_s$. The $z$-axis is taken in the spanwise direction. A measurement shows that no separation takes place on the ceiling plate opposite to the curved plate. The velocity of the main flow was varied from 1 to 5 m/s and the thickness of the boundary layer at $x = 0$ corresponding to this velocity range is from 7.0 cm to 5.3 cm. The Reynolds number based on the boundary-layer thickness covers from 5000 to 18000.

### 2.2. *Flow-visualization technique*

The flow visualization was made by smoke wires. A smoke picture with continuous ejection of smoke provides us with information about the whole flow field. The quantitative interpretation of the picture is, however, very difficult, because the picture illustrates an integrated effect on the displacement of smoke. Sometimes entirely different conclusions are drawn from one picture. In order to avoid this uncertainty we use only 'young smoke', namely, a picture is taken shortly after the smoke is released from the wire. In this case the smoke travels a short distance and we can observe instantaneous streamlines.

Each smoke wire is 50 μm diameter platinum wire about 20 cm in length. Smoke from liquid paraffin is generated by a current pulse into the wire. By using a large number of wires simultaneously, we obtain a one-shot picture of the whole flow field. As many as 31 wires were used. They were arranged in various kinds of array in the $(x, y)$- and $(x, z)$-planes. The disturbance due to this large number of wires was proved to be small by comparing single- and multiwire pictures. We can also achieve conditional visualization, in which a picture is taken when a certain condition is satisfied. The condition signal comes from a hot-wire anemometer or direction-sensitive anemometer. By means of this technique we can collect pictures under the same condition.

### 2.3. *Direction-sensitive hot-wire probe and flow-direction meter*

A hot-wire anemometer was used in the boundary layer before separation. But since it cannot distinguish the direction of the flow, it cannot be used in the separation region. Westphal, Eaton & Johnson (1981) reported the use of a three-wire probe for measurement of reversing flow. Their probe is appropriate only for the measurement near the wall.

A thermal-tuft method was developed by Ligrani *et al.* (1983), but their results are mostly qualitative. We have developed a three-wire hot-wire anemometer which distinguishes the direction of the streamwise component of velocity. A picture of the anemometer is shown in figure 2(*a*). The horizontal ($z$-wise) central wire, about 2.5 mm in length, is a conventional single hot wire. Two vertical ($y$-wise) wires are temperature-sensitive cold wires and are set at both sides of the central wire, separated from it by about 0.7 mm in the $x$-direction. The heat wake of the central

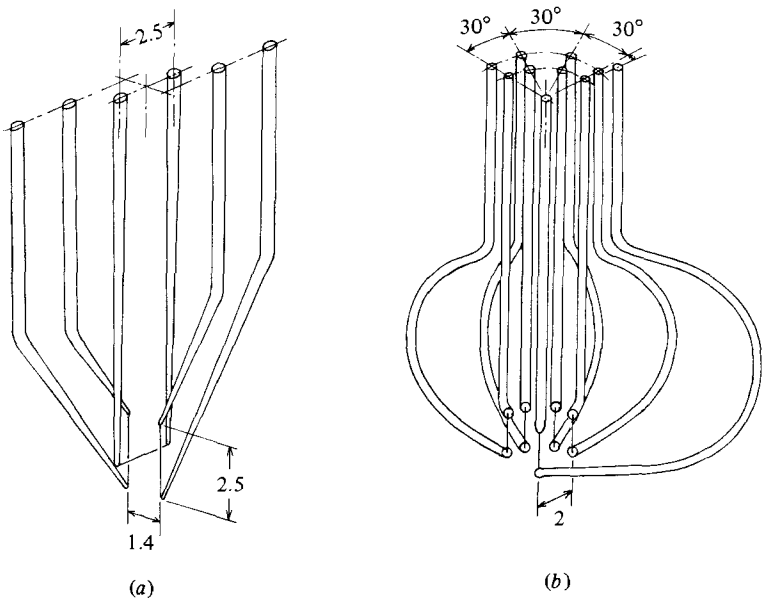


FIGURE 2. (a) Three-wire direction-sensitive hot-wire probe. (b) Flow-direction meter with four cold wires. Lengths in cm.

hot wire is picked up by either one of the wires, depending on the direction of velocity. Because the cold wires are set perpendicular to the central wire, the chance of missing the heat wake at high 'angle of attack' is small.

Outputs from two cold wires are processed and the positive or negative sign of the velocity is obtained. If $u = 0$ neither cold wire produces output and the velocity is registered as zero. This processing means that the magnitude measured by the hot wire is $(u^2 + nv^2)^{\frac{1}{2}}$, with $n$ slightly smaller than one. Experimental results indicate that the fraction of time in which $u = 0$ is at most 5% of the total time period. Another problem associated with the anemometer is the effect of the wake of a cold-wire support. When $u > v$ the hot wire is in the wake of a cold wire and the effect is very small. When $u \ll v$ the hot wire is on the wake of cold-wire support. Then the hot wire picks up a velocity fluctuation in the wake, but the scale of the fluctuation is small. Since in the present experiment we are mostly interested in large-scale fluctuations, the effect of the support wake can be ignored. The hot wire is operated in the constant-temperature mode. The output is linearized in the wind-speed range from 0.4 to 5 m/s. Measurements at speeds less than 0.4 m/s are not accurate. Two identical three-wire probes were used for the measurement of the spatial correlation of the occurrence of backflow.

In the central part of the separated region the flow direction changes by 360°. Since this change is too large to be measured by the three-wire probe, we have developed a flow-direction meter. It consists of a heater and many cold-wire temperature sensors around the heater. The heated wake of the central heater is detected by the cold wires, and the flow direction is determined by the position of the cold wire which produces the temperature signal. Usually temperature signals come from two or three adjacent cold wires. The instantaneous flow direction is determined by an adequate processing of these signals. The flow direction in the $(x, z)$-plane was measured by a direction meter with five wires. A picture is shown in figure 2(b). A heater, 2 mm in length, is set in the $y$-direction and four parallel cold

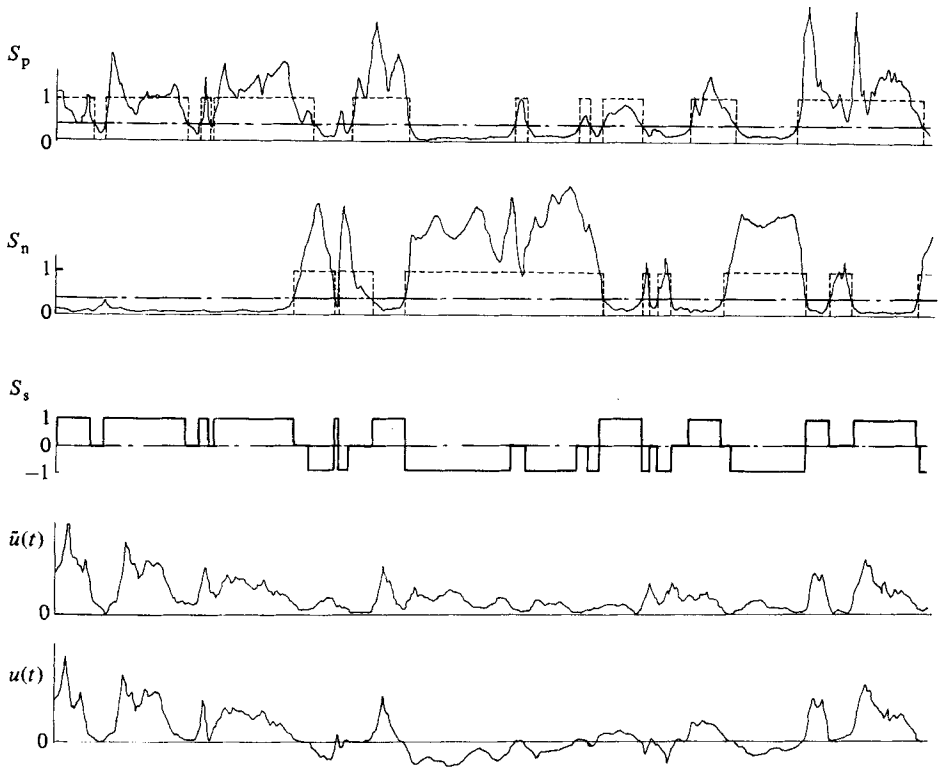


FIGURE 3. Processing of output from direction-sensitive probe. $S_p \equiv$ forward-flow signal, $S_n \equiv$ backflow signal; $S_s \equiv$ sign signal, $\hat{u}(t) \equiv$ output from hot wire, $u(t) \equiv$ velocity with sign.

wires are placed on the circle of 2 mm radius, 30° apart from each other. The whole assembly can be rotated around the heater. It permits the measurement in 360°. The flow direction in the $(x, y)$-plane was measured by an eight-wire direction meter which has seven cold wires around one heater. The principle of operation is the same as the five-wire meter. Since these meters are not small enough, we can measure only large-scale fluctuations. The probability-density distribution of the flow direction, 'wind rose', is obtained from these direction meters.

### 2.4. *Data manipulation*

Experimental data obtained by the various methods were processed in various ways by a laboratory minicomputer. Smoke pictures taken under the same condition are reproduced by a TV camera and the displacement of smoke is measured and stored in the memory of the computer. Then quantities such as correlation are computed. This is a statistical processing of picture information.

Figure 3 illustrates how the signed instantaneous velocity is obtained from outputs of the three-wire direction-sensitive anemometer. Outputs from the downstream and upstream cold wires are converted to a 0, 1 signal by an appropriate amplitude threshold which is shown by an chain line. Converted signals $S_p$ and $S_n$ are shown by broken lines. The sign signal $S_s$ is defined as $S_s = 1$, when $S_p = 1$, $S_n = 0$, and $S_s = -1$ when $S_p = 0$, $S_n = 1$. As shown in the figure, at some instants both $S_p$ and $S_n$ are 1 or 0 simultaneously. In this case we cannot distinguish the direction of flow. So we set $S_s = 0$. The measurement shows that the fraction of time for which $S_s = 0$

is less than 10 % of the total time interval. Therefore the error due to this ambiguity is small. We multiply the hot-wire signal $\hat{u}(t)$ by $S_s$ and obtain the velocity with sign, $u(t)$. Statistical quantities are computed with this signed velocity. As mentioned before this velocity is not exactly the velocity component in the $x$-direction. But for simplicity we designate the velocity picked up by the hot wire as $u(t)$. The sign signal itself is a significant physical quantity. We compute the correlation of two sign signals from two direction-sensitive anemometers in the flow. We can also use the signal as a condition for sampling. The backflow factor $R_n$ is defined as the fraction of occurrence of backflow in the total time interval of measurement.

The conditional sample-and-average technique is very useful. We can obtain the conditional backflow factor. We set a threshold for the instantaneous $u$-signal from a hot-wire anemometer in the upstream boundary layer and sample the sign signal when $u$ crosses the threshold. It is possible to set positive or negative time lag; that is, the sign signal is sampled some time before or after the condition is satisfied. From the conditional sign signal we compute the conditional backflow factor. We can work the other way around; that is, we set a condition by the sign signal and sample the velocity in the upstream boundary layer. It indicates what happens in the upstream boundary layer before and after intermittent backflow occurs on the downstream curved surface.

## 3. Experimental results

### 3.1. *Smoke pictures*

Figure 4 shows a picture of smoke from 31 wires. All wires are arranged normal to the flow and parallel to the wall with the same distance from the wall.

The width of the array is 20 cm. In the flow direction the array covers about 20 cm on the flat plate and 40 cm on the curved wall. The distance from the wall is 0.5 cm for (*a*) and 2 cm for (*b*), which corresponds to $y_s/\delta_0 = 0.07$ and 0.3 respectively. The 99 % thickness of the boundary layer at $x = 0$ is denoted by $\delta_0$. The front of each smoke represents the instantaneous velocity. Fine streaky lines in each smoke indicate the direction of flow. Figure 4 (*a*) shows low-speed and high-speed lumps of fluid on the flat plate. They are elongated in the flow direction. The flow is decelerated on the curved wall, and at around $x = 12$ cm localized backflows take place. They form backflow 'spots', which grow downstream. At around $x = 25$ cm most of the surface is covered by backflows. In (*b*) the lateral non-uniformity is smaller and the backflow takes place at larger $x$. In the 'fully developed' backflow region there is not much difference between (*a*) and (*b*).

Figure 5 shows smoke pictures with two arrays of smoke wires, which are arranged in horizontal and vertical planes. Eight horizontal wires are placed at $y_s/\delta_0 = 0.2$ in the top view. They show the $u$-component as a function of $z$ at various $x$-stations. In the side view eight wires are set vertically. They show $u$ as a function of $y_s$. Smoke is released simultaneously from all wires and pictures are taken by two cameras from two directions. A hot-wire anemometer is placed in the field as seen in both pictures. Pictures are taken when a low-speed lump of fluid hits the hot-wire. These two pictures show the three-dimensional structure of a low-speed lump on the flat plate.

Figure 6 is a smaller picture taken on the curved wall between $x = 20$ and 30 cm. The condition for this figure is the backflow signal from a direction-sensitive hot wire shown in the picture. Smoke patterns from vertical wires show the velocity distribution with a backflow, and the same backflow is seen in the centre of the top view. The backflow region is elongated in the flow direction and short in the $z$-direction.

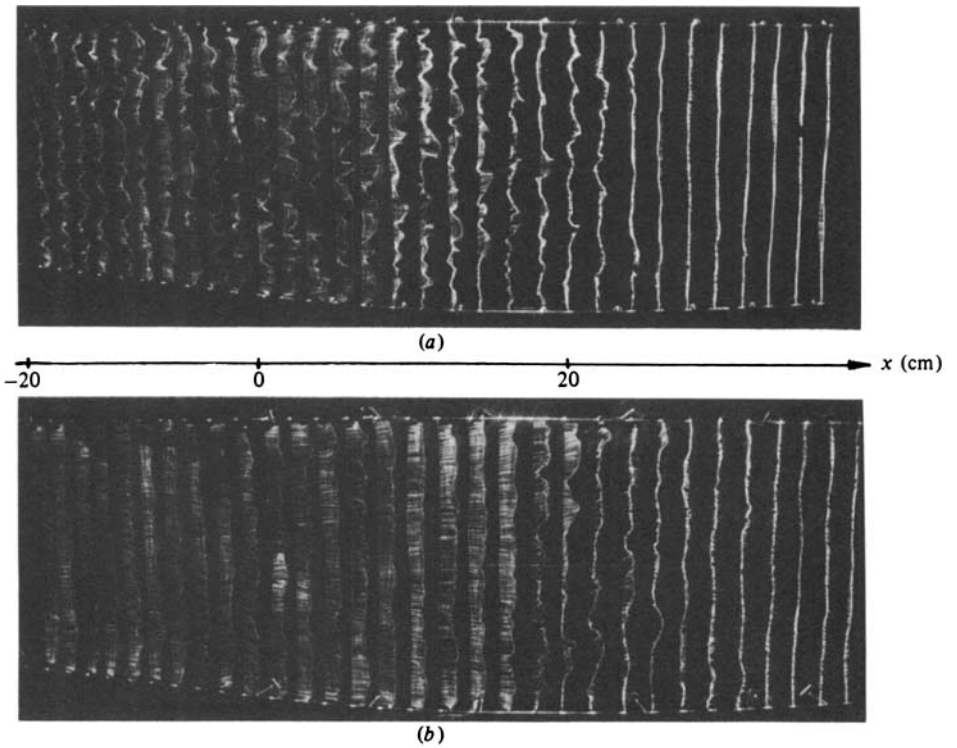


FIGURE 4. Smoke-wire pictures at 31 stations: (*a*) location of smoke wires 0.5 cm from the wall; (*b*) location of smoke wires 2 cm from the wall. $U_0 = 1$ m/s, flow from left to right.

Figure 7 shows a smoke picture taken by a horizontal three-layer wire array. Wires are placed at three different positions from the wall. Each array consists of 8 or 9 parallel smoke wires. By this arrangement we can observe the three-dimensional structure of instantaneous backflow. Each array of wires is constructed in a flat plane; therefore the array is not parallel to the curved wall. The distance of the wire from the wall at the downstream end is about 40 % greater than that at the upstream end. The picture is complicated because many smoke sheets overlap. By careful tracing we can separate each sheet and reconstruct a smoke picture as shown in figure 8. From this figure we observe that a backflow near the wall is frequently accompanied by a low-speed lump at large distance from the wall.

### 3.2. *Mean and fluctuating velocities*

Two most important statistical properties of the turbulent flow are the mean velocity $U$ and the intensity of fluctuation $(\overline{u^2})^{\frac{1}{2}}$. Figure 9 shows distributions of the mean velocity at various $x$-stations with $U_0 = 3$ m/s. Data were obtained by the direction-sensitive hot-wire anemometer, the output of which was processed as explained in §2. In the figure the mean velocity on a flat plate shows a familiar turbulent boundary-layer-type distribution. The distribution does not change much in the flow direction until $x = 15$ cm. At $x = 20$ cm the boundary layer becomes thicker and the velocity gradient at the wall becomes smaller. At $x = 30$ cm the gradient is almost zero, and at around $x = 40$ cm a region of negative mean velocity is formed. The region exists up to 70 cm and disappears at around $x = 95$ cm. The reattachment takes place there. The inflection point in the distribution first appears at $x = 30$ cm.

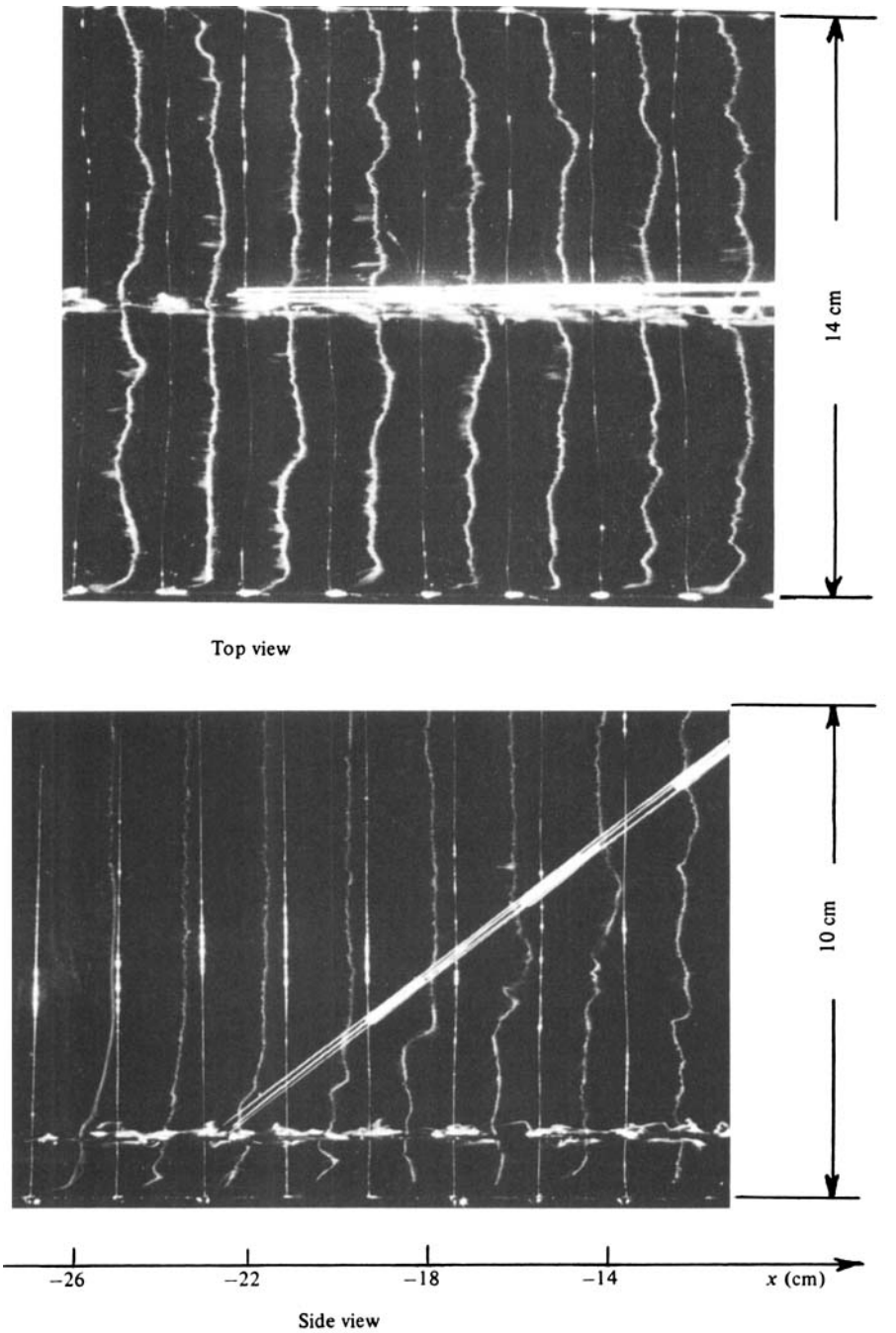


FIGURE 5. Simultaneous top and side views of smoke on the flat plate. A hot-wire anemometer is placed at $x = -23$ cm, $y = 1.5$ cm. Distance between wires = 2 cm, $U_0 = 1$ m/s.

The point first moves away from the wall as $x$ is increased, and later approaches the wall again. The thickness of the reattached boundary layer is more than twice that of the original boundary layer.

Distributions of the intensity of fluctuation are shown in figure 10. On the flat plate a familiar distribution is found. It is noted that outside the boundary layer $(\overline{u^2})^{\frac{1}{2}}$ is

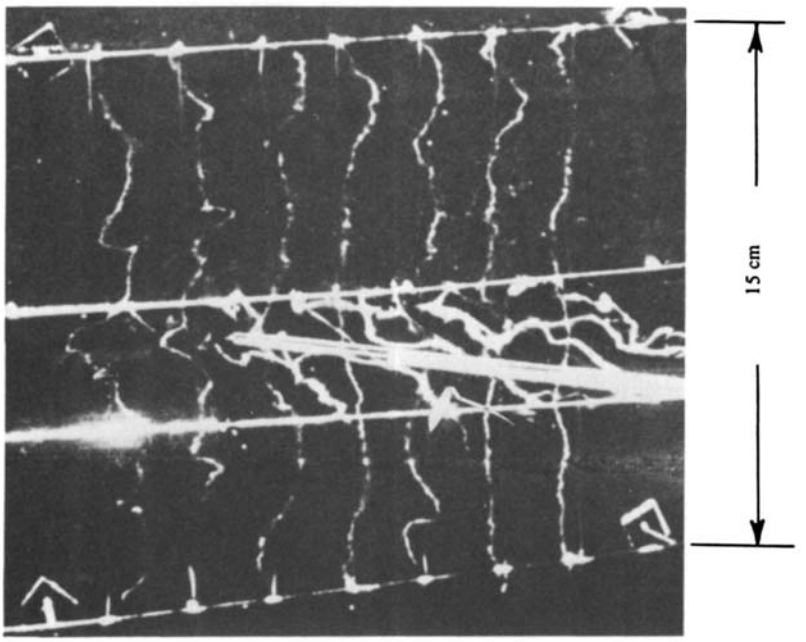


Top view

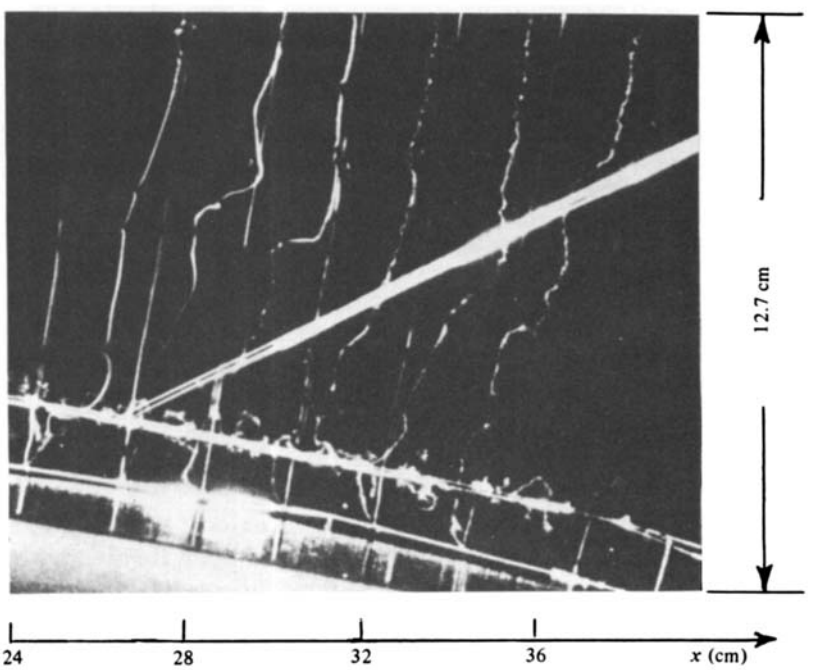


Side view

FIGURE 6. Simultaneous top and side views of smoke on the curved wall. A direction-sensitive hot-wire probe is placed at $x = 25$ cm, $y = 1.5$ cm. Distance between wires = 2 cm, $U_0 = 1$ m/s.

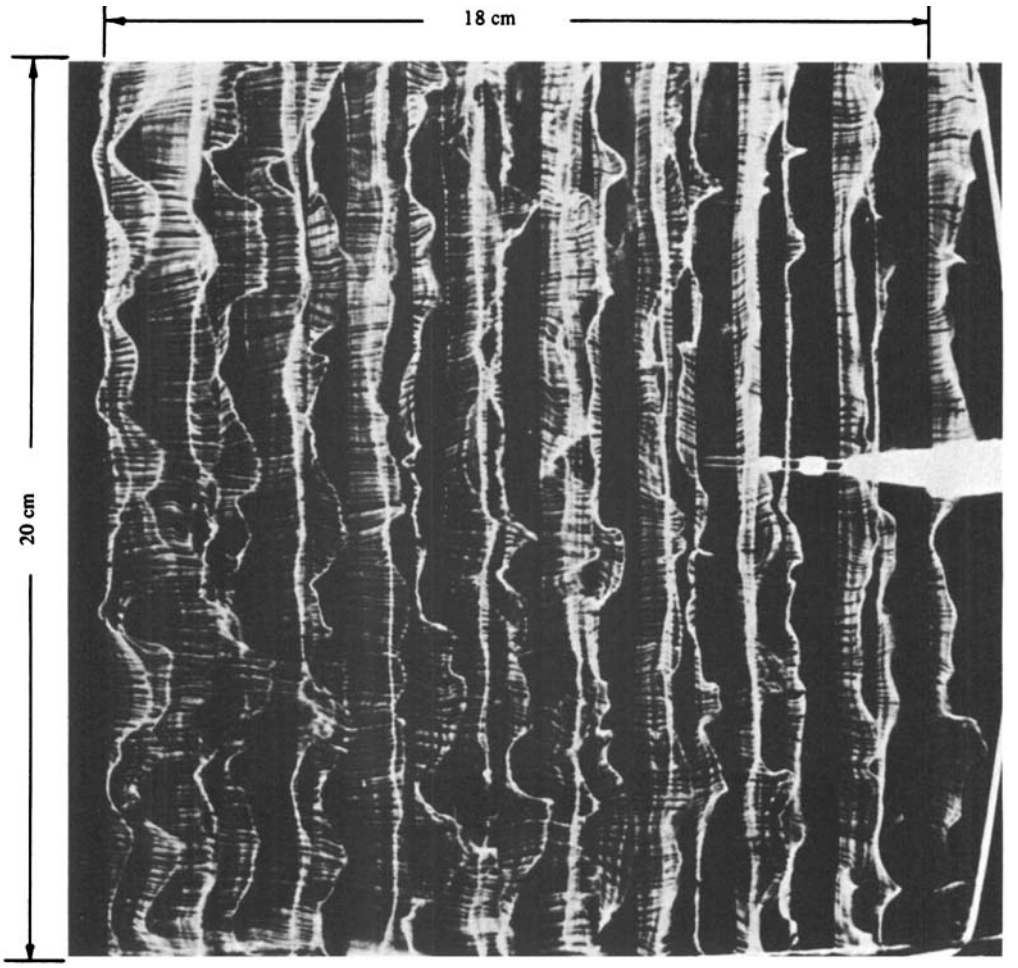


FIGURE 7. Smoke-wire pictures using three-layer wire arrays. Distance from the wall at upstream end, 1 cm, 2 cm, and 3 cm, $U_0 = 1$ m/s.

about 2% of $U_0$. The distribution changes in accordance with the mean-velocity distribution; namely the high intensity is found at large gradient of mean velocity. The maximum fluctuation level reaches 15%. It is impossible to find any similarity in the distributions of $U$ or $(\overline{u^2})^{\frac{1}{2}}$ at various $x$-stations.

### 3.3. *Backflow factor and wind rose*

The backflow factor $R_n$ (the fraction of occurrence of backflow in the total time of measurement) is shown in figure 11. On the flat plate there is no backflow, that is, $R_n = 0$. A small backflow region appears at around $x = 20$ cm near the wall. The mean velocity at the $x$-station is still positive everywhere as shown in figure 9. We cannot find any sign of backflow in the mean-velocity distribution. The backflow factor increases downstream, and at around $x = 40$ cm the maximum value near the wall is close to unity; namely, the flow there is always in the negative direction. The broken line in the figure connects points of $R_n = 0.01$. The region surrounded by the line and the wall may be called the separated region, although in a strict sense the backflow and the separated flow are different concepts. The chain line connects points of

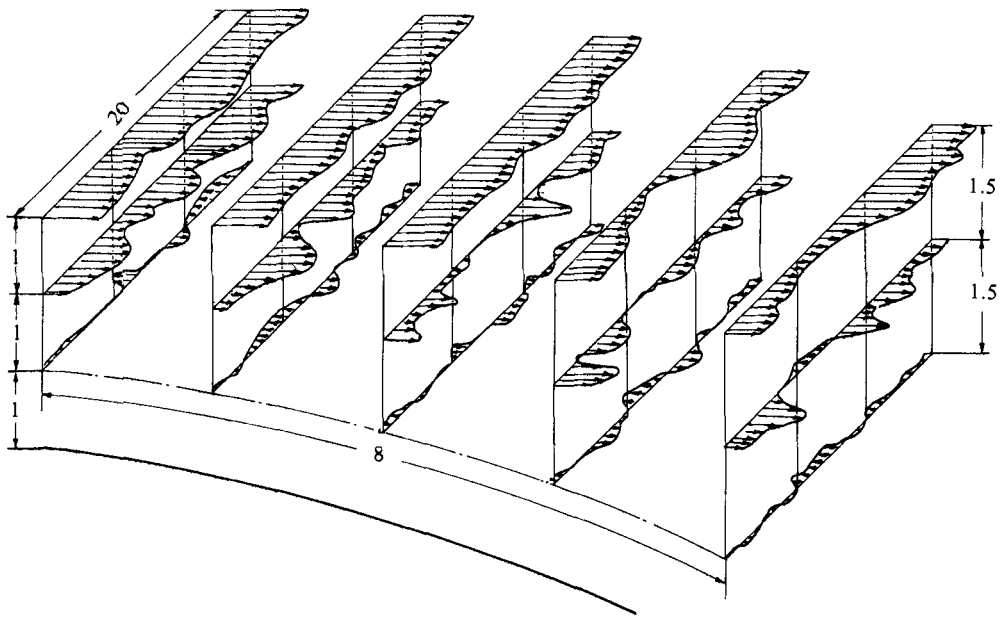


FIGURE 8. Reconstructed three-layer smoke pictures on the curved wall; length in cm.

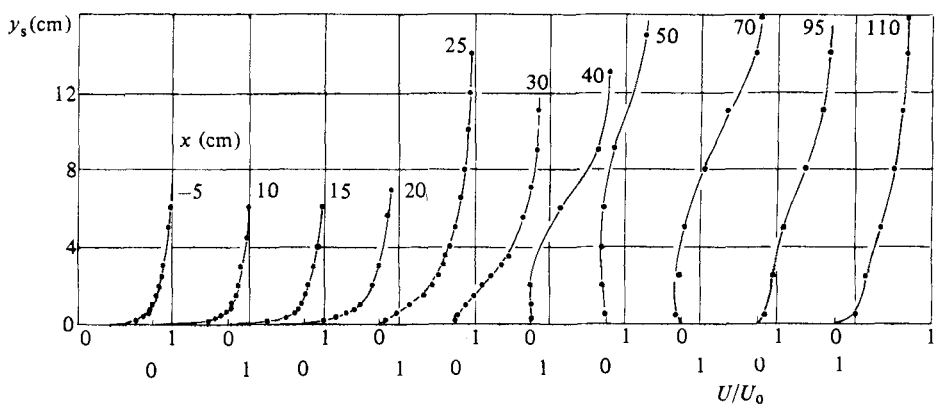


FIGURE 9. Mean-velocity distributions; $U_0 = 3$ m/s.

$R_n = 0.5$. Inside the line the backflow is more frequent than the forward flow. It is interesting to note that at $x = 50$ cm the factor is less than unity very close to the wall. This suggests that a small forward flow is formed at the corner. At about $x = 120$ cm $R_n$ becomes zero again. This place is the downstream end of occurrence of backflow. Comparing distributions of mean velocity and backflow factor, we notice two facts. First, the line of $R_n = 0.01$ almost coincides with the line connecting inflection points in the mean-velocity distribution. Secondly, the line of $R_n = 0.5$ passes through points of $U = 0$. The first result may be related with the presence of a maximum in fluctuation amplitude at the inflection point, and this large amplitude-fluctuation may eventually result in an instantaneous backflow. The second fact suggests that the forward and backward flows are statistically similar. The measured probability distribution of fluctuation amplitude confirms the similarity.

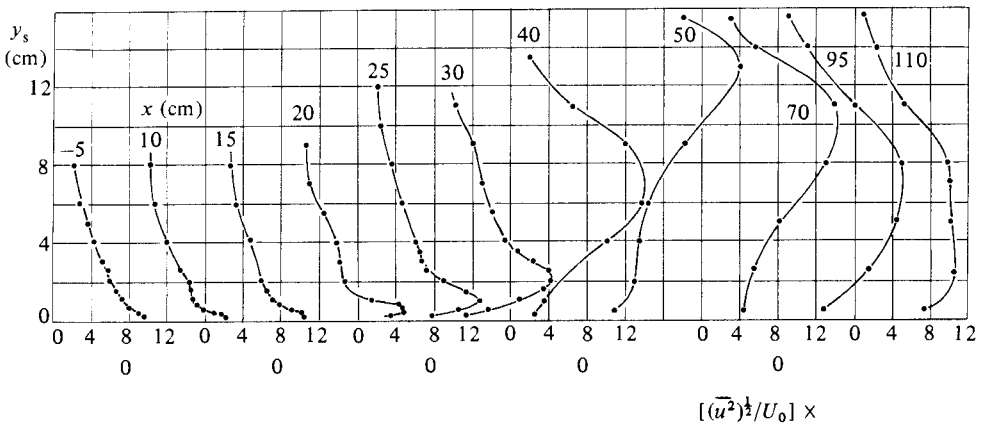


FIGURE 10. Distributions of fluctuation intensity; $U_0 = 3$ m/s.

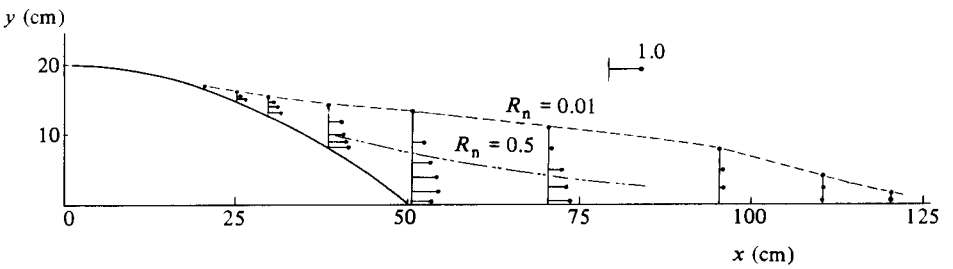


FIGURE 11. Distribution of backflow factor; $U_0 = 3$ m/s.

Figure 12 shows wind roses measured in two planes by the use of flow-direction meters. The number of occurrences is indicated by the length of arrow. In the vertical $(x, y)$-plane the flow at $y_s = 11$ cm is predominantly in the 4 o'clock direction, which is nearly parallel to the convex surface. At $y_s = 9$ cm a strong 5 o'clock component and a small backflow component are observed. The backflow component becomes large as the probe comes closer to the wall. Components normal to the wall are strong between $y_s = 7$ cm and 5 cm. At $y_s = 3$ cm the backflow parallel to the wall is predominant. The strong vertical components around $y_s = 5$ cm seem to indicate the existence of a two-dimensional vortex with the axis in the $z$-direction. Wind roses measured in the horizontal $(x, z)$-plane, however, indicate a strong three-dimensional nature of velocity fluctuations. For instance, it is almost impossible to imagine a two-dimensional vortex from the wind rose in the horizontal plane measured at $y_s = 5$ cm. If a two-dimensional vortex exists, the wind rose must consist of predominant 3 o'clock and 9 o'clock components. But there are strong lateral components. All wind roses in the horizontal plane are symmetrical with respect to the $x$-axis. This means that, in the average, the flow is two-dimensional. Wind roses measured at different $x$-stations are similar to those shown in figure 12.

### 3.4. *Correlations and conditional averages*

Various correlations were measured for clarifying the spatial and temporal structures. One is the lateral correlation of $u$-fluctuation in the boundary layer ahead of the separation. This is obtained by the statistical processing of smoke pictures. At each $x$-station about 20 smoke pictures like figure 4 are processed by a minicomputer. The

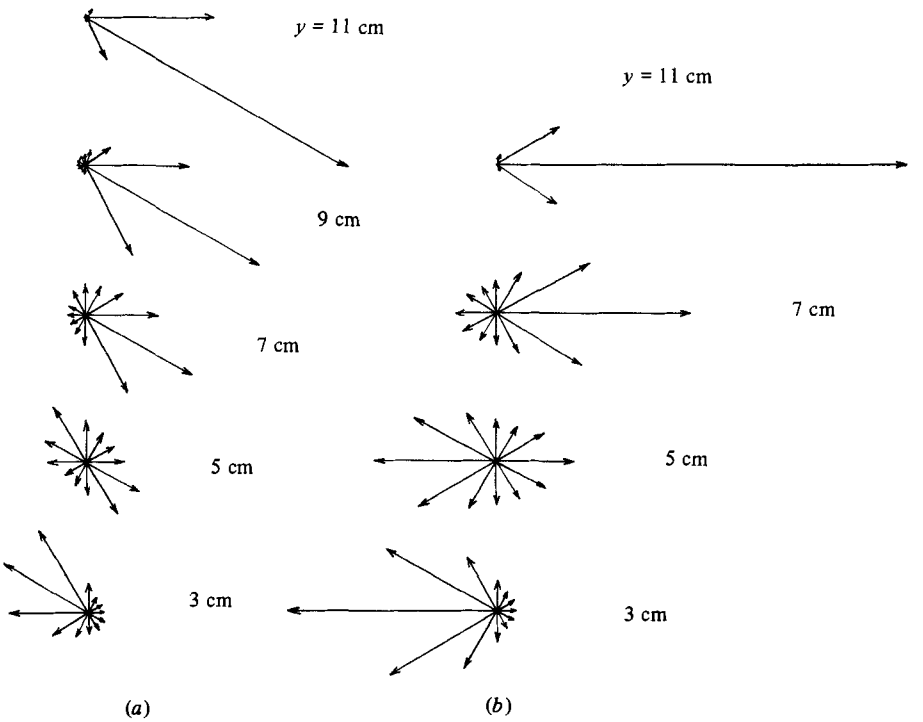


FIGURE 12. Wind roses at $x = 50$ cm; (*a*) in the $(x, y)$-plane; (*b*) in the $(y, z)$-plane.

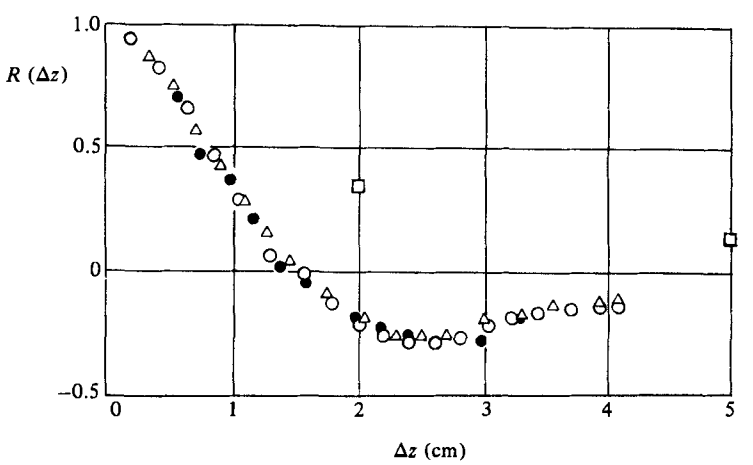


FIGURE 13. Lateral correlations of $u$-fluctuations; $U_0 = 1$ m/s, $y/\delta_0 = 0.3$: ○, $x = -10$ cm; ●, 0; △, 10 cm; □, correlation of backflow signal, $x = 35$ cm, $y_s = 0.5$ cm.

correlation near the wall is obtained as a function of $\Delta z$ as shown in figure 13. This is a correlation of large-scale fluctuations, because in the course of processing small-scale fluctuations are ignored. Curves at three $x$-stations are almost identical. The negative correlation at large $\Delta z$ reflects the fact that narrow high-speed and low-speed lumps exist side by side near the wall. The average width of each lump is about 3 cm, which is about half the thickness of the boundary layer. The lateral extension of the instantaneous backflow region is expressed by the correlation of

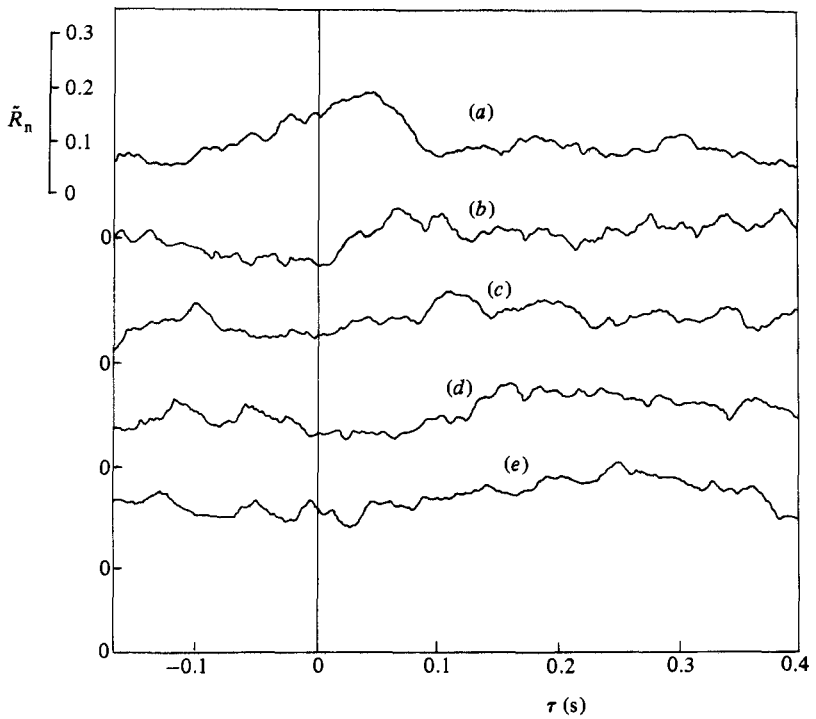


FIGURE 14. Conditionally averaged backflow factor $\tilde{R}_n$; $U_0 = 3$ m/s. Location of direction-sensitive probe; $x = 24.4$ cm, $y_s = 0.3$ cm. Locations of hot wire: (*a*) $x = 18.9$ cm, $y_s = 1.1$ cm; (*b*) 15 cm, 1.4 cm; (*c*) 11 cm, 1.2 cm; (*d*) 5 cm, 0.9 cm; (*e*) −5 cm, 0.7 cm. $\tau \equiv$ delay time.

backflow signals $S_n$ in the $z$-direction. The correlation is added in figure 13. The backflow factor at the point is 0.30. Therefore the maximum value of the correlation is 0.3 and the value for uncorrelated signal is 0.09. The relation between velocity correlation and backflow-signal correlation will be discussed in §4.

The next quantity is the streamwise correlation. The conditional backflow factor explained in §2.4 is shown in figure 14. The direction-sensitive probe was fixed at $x = 24$ cm and the condition hot-wire anemometer was moved from $x = 19$ cm to $x = -5$ cm. A condition signal is generated when the flow velocity becomes smaller than the preset threshold; namely when a low-speed lump of fluid passes through the hot wire. The condition signal is delayed and the conditional backflow factor is obtained as a function of the delay time $\tau$. The positive delay time indicates that the event takes place after the condition signal is generated. Since the threshold for the velocity signal is rather arbitrary, the absolute value of the conditional backflow factor is not important. We notice a peak in each curve. For instance, in curve (*b*) there is a peak at a delay time of around +0.1 s. As the condition hot wire is moved upstream, the peak becomes less distinct, but we still observe that the delay time corresponding to the peak increases. This means that a low-speed lump observed at an upstream position travels downstream and causes a backflow.

Examples of conditional mean velocity obtained as described in §2.4 are shown in figure 15. In this case the direction-sensitive probe generates the backflow signal which is used as a condition. The velocity is ensemble-averaged with delay time. The negative delay time indicates that the event takes place before the condition signal is generated. In each curve we observe a minimum. This indicates that a low-speed lump passes through the hot wire some time before the backflow takes place

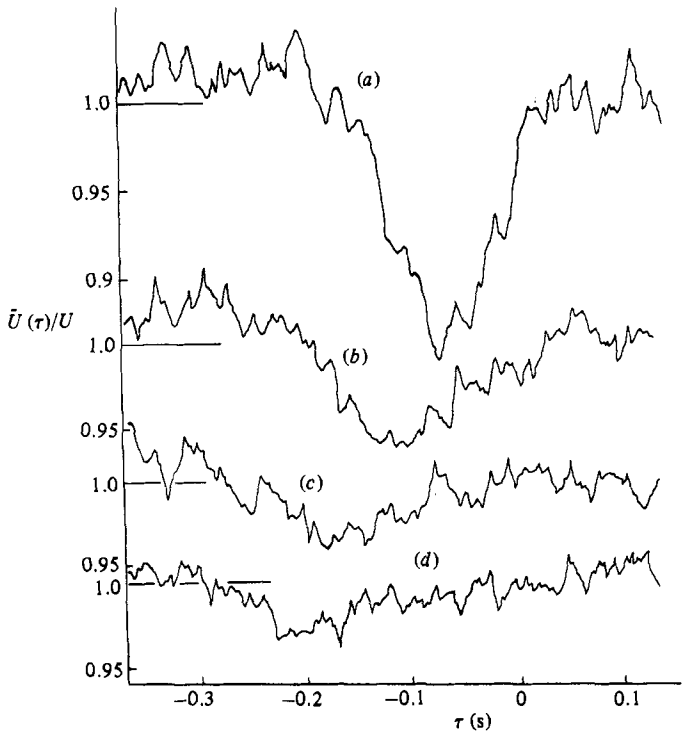


FIGURE 15. Conditionally averaged velocity. Location of direction-sensitive probe: $x = 25.4$ cm, $y_s = 0.3$ cm. Locations of hot wire; (*a*) $x = 19.8$ cm, $y_s = 0.6$ cm; (*b*) 15 cm, 0.6 cm; (*c*) 10 cm, 0.6 cm; (*d*) 5 cm, 0.6 cm. $U_0 = 3$ m/s; $\tau \equiv$ delay time.

downstream. As the hot wire is moved upstream the negative time delay for the minimum averaged velocity increases. This fact confirms that the occurrence of backflow is closely connected with the existence of a low-speed lump upstream. The propagation speed, or 'celerity', of the low-speed lump is estimated as about $0.4U_0$.

## 4. Discussion

First of all we try to define the word 'separation'. In general, separation is a process in which something attached to a solid wall moves away from it. We apply this definition to the flow of fluid. In the turbulent boundary layer small fluid particles move up and down and some of them may eventually move away from the wall. But this is not separation. It is a small-scale motion in the turbulent flow. Separation must be a large-scale motion. However, as we have seen in §3, the occurrence of backflow is local in space and intermittent in time. Is there then any appropriate scale for defining the separation? The answer is no, and is impossible to find such a scale. Thus the precise definition of instantaneous separation is impossible. Therefore in the following discussion we may not use the word 'separation' except when the work with a vague definition is still useful.

### 4.1. *Flat-plate boundary layer*

Distribution of mean velocity and intensity of fluctuation of the boundary layer along the flat plate observed in the present experiment are the same with many other experimental results, except that there is about 2 % turbulence in the main flow. The

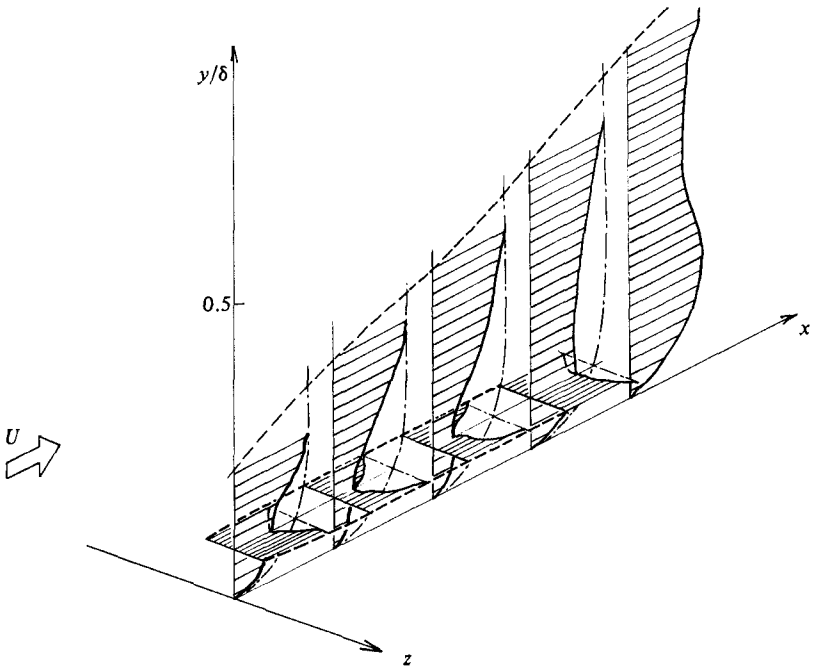


FIGURE 16. Sketch of low-speed lump on the flat plate: —·—·, time-averaged velocity; ——, conditionally averaged velocity; – – –, outline of lump.

effect of this weak fluctuation on the separation might be small, because much stronger fluctuations exist in the boundary layer.

Smoke pictures in the boundary layer, such as figures 4 and 5, provide useful information. Top views shown many low-speed and high-speed lumps which are narrow in the $z$-direction and elongated in the $x$-direction. Obviously they are large-scale ordered motions. The side view in figure 5 clearly shows complicated instantaneous velocity distributions in the $y$-direction. As many as three inflectional points are found. From a large number of conditional smoke pictures we can construct an average low-speed lump as shown in figure 16. Chain lines show time-averaged velocity distributions and full lines show conditionally averaged velocity distributions in the $y$- and $z$-directions. The shaded area illustrates a low-speed lump. The width of the lump in the $z$-direction is around $0.1$–$0.2\,\delta$.

The maximum height is about $0.5\delta$ and the length is about $\delta$. This pattern is very close to those obtained by many investigators of ordered motions.

### 4.2. *Structures of backflow region*

Figure 4 shows an instantaneous flow field with backflow. Figure 17 is a map of the backflow region. The shaded area illustrates the backflow 'spots' or 'wedges'. They are irregular in shape, grow in the flow direction and merge with each other. This process is similar to the development of turbulent spots in the transition region of a boundary layer. The backflow factor corresponds to the intermittency factor. One difference is that the backflow spots do not have any definite shape as turbulent spots do. The broken line indicates the upstream limit of occurrence of backflow. It may be called the 'backflow front'.

The lateral correlation in figure 13 shows that the total width of a low-speed lump

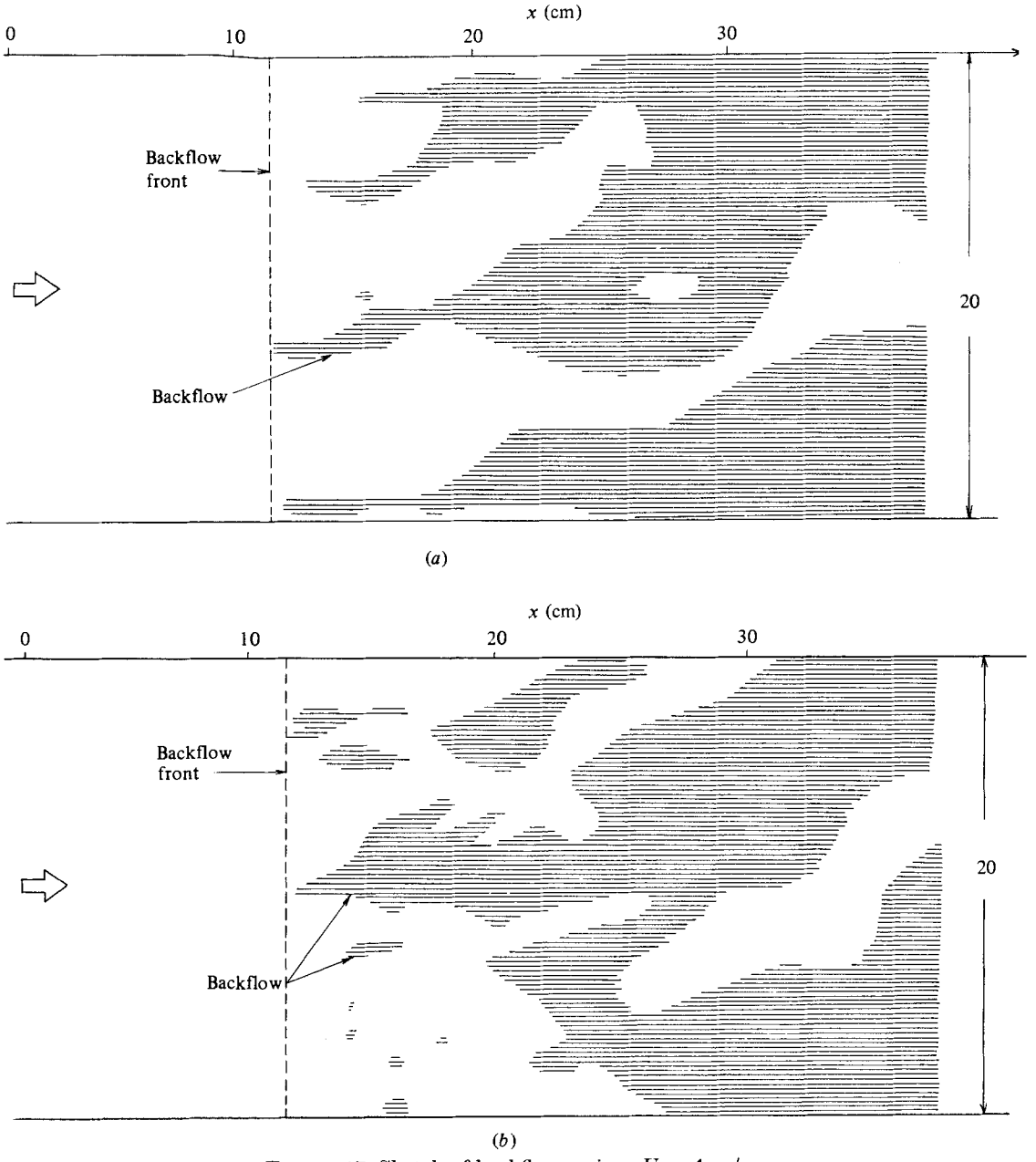


FIGURE 17. Sketch of backflow region; $U_0 = 1$ m/s.

of fluid is about 2 cm on the flat plate. The lateral scale of the backflow region can be estimated from the measurement of correlation of backflow signal in the $z$-direction. One example is shown in the same figure. Since the backflow signal takes values 0 and 1, the correlation is a little different from that of a continuous positive/negative signal. From the figure we observe that the two scales are not very different.

The detailed structure of the backflow region is clearly demonstrated in figure 8. At the lowest layer, which is about $0.15$–$0.20\,\delta_0$, backflows occur frequently. A tall backflow region extends to the middle layer of about $0.3$–$0.4\,\delta_0$. But a short backflow

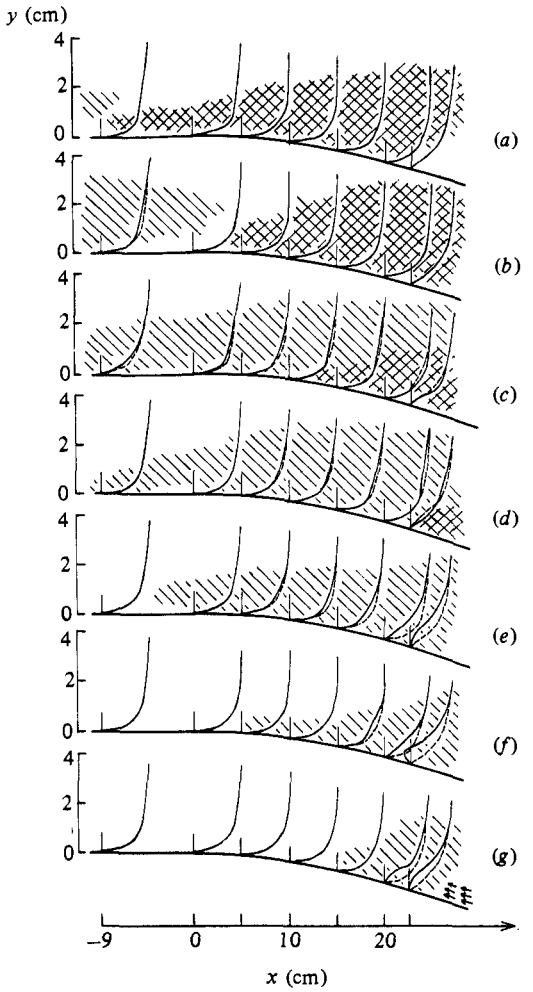


FIGURE 18. Sequence of conditionally observed velocity. Location of direction-sensitive probe: $x = 25.4$ cm, $y_s = 0.3$ cm. Delay time; (*a*) 365 ms; (*b*) 300 ms; (*c*) 235 ms; (*d*) 170 ms; (*e*) 100 ms; (*f*) 33 ms; (*g*) 0. ----, time-averaged velocity; ——, conditionally averaged velocity. Cross-hatching, high-speed lump; shading, low-speed lump.

region does not reach the middle layer. At the height of $0.4$–$0.6\,\delta_0$ there is no backflow, but there are low-speed regions. Most of them are accompanied by backflow regions at smaller $y$.

The shapes of the backflow regions show a good deal of variety, but they are neither very thick nor very thin. In other words, the scales in the $y$- and $z$-directions are about the same. As the scale in the $z$-direction increases downstream so does the scale in the $y$-direction. Although the 'grown-up' backflow region is a large-scale motion, it is difficult to claim that the motion is 'ordered'.

### 4.3. *Initiation of backflow*

The next problem is the initiation of backflow. Figures 14 and 15 indicate that the passage of a low-speed lump upstream and the occurrence of backflow downstream are closely correlated with a certain time lag. We made more detailed measurements on this point. The occurrence of backflow at a test point, $x = 22$ cm, was used as a

condition, and the conditional average of flow velocity in the upstream region was made. We wanted to know what happens upstream before a backflow occurs. The result is shown in figure 18. It includes distributions of conditionally averaged velocity with seven negative delay times. These distributions illustrate the history of the flow field. Broken lines indicate non-conditional averages. Shading and cross-hatching indicate low-speed and high-speed lumps of fluid respectively. At $-360$ ms most of the field is covered by a high-speed lump. A small low-speed lump appears far upstream. As time goes on, the high-speed lump moves downstream. At $-165$ ms most of the high-speed lump passes through the test point and the low-speed lump surrounds it. At $-100$ ms there is no high-speed lump any more. Although the test point is swept by the low-speed lump, no backflow appears yet. At time zero the low-speed lump passes through the point and a backflow appears. We should keep in mind that this is an average picture. Each initiation of the backflow may not be exactly the same. An interesting point is the role of the high-speed lump. It is not probable that the lump initiates the backflow. The possibility is that a high-speed lump is a precursor of a low-speed lump in the turbulent boundary layer. This combined large-scale ordered motion does initiate a local and intermittent backflow. The high freestream turbulence in the present experiment may modify the structure of the boundary layer a little, but the fundamental feature of separation may not be affected.

The onset of backflow depends on two factors. One is the pressure distribution. If the adverse pressure gradient in the flow direction is large, then the flow is decelerated greatly and a low-speed lump can easily be converted into a backflow region. The other factor is the 'strength' of ordered motion in the original boundary layer. If low-speed lumps in the layer are strong then the backflow takes place at small $x$. We may be able to control the turbulent separation by modifying ordered motions in the boundary layer.

## 5. Concluding remarks

Visual observations by smoke wires and measurements by various kinds of hot-wire probe indicate the following conclusions.

1. In the boundary layer along a flat plate smoke pictures reveal that low-speed lumps and high-speed lumps of fluid exist side by side near the wall. They extend in the flow direction, and in an average sense a high-speed lump moves downstream in front of a low-speed lump.

2. The backflow region on a curved wall is described by a new statistical quantity, the backflow factor, which is defined as a fraction of time covered by the backflow.

3. Backflow spots are observed by smoke pictures. They are localized in space and intermittent in time. The spots grow downstream, merge with each other and finally cover the whole surface of the curved wall.

4. There are similarities between the backflow in the separation region and the turbulent spot in the transition region. The difference is that the backflow spot does not have a definite shape.

5. Wind roses in the separation region illustrate a strong three-dimensionality. The model of a lateral vortex in the separation region is not adequate for the turbulent separation.

6. The time sequence of backflow is clarified by the conditional averaging. A backflow is initiated by a low-speed lump of fluid which moves down along the curved wall.

## REFERENCES

LIGRANI, P. M., GYLES, B. R., MATHIOUDAKIS, K. & BREUGELMANS, F. A. E. 1983 *J. Phys.* E: *Sci. Instrum.* **16**, 431.

SANDBORN, V. A. & KLINE, S. J. 1961 *Trans. ASME* D: *J. Basic Engng* **83**, 317.

SHILOH, K., SHIVAPRASAD, B. G. & SIMPSOM, R. L. 1981 *J. Fluid Mech.* **113**, 75.

SIMPSON, R. L., STRICKLAND, J. H. & BARR, P. W. 1977 *J. Fluid Mech.* **79**, 553.

SIMPSON, R. L., CHEW, Y.-T. & SHIVAPRASAD, B. G. 1981*a* *J. Fluid Mech.* **113**, 53.

SIMPSON, R. L., CHEW, Y.-T. & SHIVAPRASAD, B. G. 1981*b* *J. Fluid Mech.* **113**, 75.

WESTPHAL, R. V., EATON, J. K. & JOHNSON, J. P. 1981 *Trans ASME* I: *J. Fluids Engng* **103**, 431.